A Journal of the Gesellschaft Deutscher Chemiker

Angewandte International Edition

GDCh

Chemie

www.angewandte.org

Accepted Article

Title: Irreversible amide-linked covalent organic framework for selective and ultrafast gold recovery

Authors: Hai-Long Qian, Fan-Lin Meng, Cheng-Xiong Yang, and Xiu-Ping Yan

To be cited as: *Angew. Chem. Int. Ed.* 10.1002/anie.202006535

Link to VoR: https://doi.org/10.1002/anie.202006535

WILEY-VCH

10.1002/anie.202006535

WILEY-VCH

Irreversible amide-linked covalent organic framework for selective and ultrafast gold recovery

Hai-Long Qian,*[a,c] Fan-Lin Meng,[c] Cheng-Xiong Yang,[e] and Xiu-Ping Yan*[a,b,c,d]

Abstract: Design of stable adsorbents for selective gold recovery with large capacity and fast kinetics is of great challenge, but significant for economy and environment. Here, we show the design and preparation of an irreversible amide-linked covalent organic framework (COF) JNU-1 via a building block exchange strategy for efficient recovery of gold. JNU-1 was synthesized through the exchange of 4,4'-biphenyldicarboxaldehyde (BA) in mother COF TzBA consisting of 4,4',4''-(1,3,5-triazine-2,4,6-triyl)trianiline (Tz) and BA with terephthaloyl chloride. The irreversible amide linked JNU-1 gave good stability, unprecedented fast kinetics, excellent selectivity and outstanding adsorption capacity for gold recovery. X-ray photoelectron spectroscopy along with thermodynamic study and quantum mechanics calculation reveals that the excellent performance of JNU-1 for gold recovery results from the formation of hydrogen bonds C(N)-H···Cl and coordinate interaction of O and Au. The rational design of irreversible bonds as both inherent linkage and functional groups in COFs is a promising way to prepare stable COFs for diverse applications.

Introduction

Though best-known as jewelry, gold actually possesses wide application in our daily life including electronics, medicine, and catalysis due to its superb physical and chemical properties.[1] The huge consumption of gold leads to the low abundance of this raw metal recourse and massive risk in ecology. Hence, the recovery of gold from secondary resources such as the waste of electrical and electronic equipment demonstrates extreme importance in view of the economy and environment.[2] Plenty of technologies involving adsorption, precipitation, solvent extraction and ion exchange have been developed to recover gold from aqueous solution.[3] The adsorption approach with porous adsorbents attracts wide attention on account of its eco-friendship, low cost, and easy operation.

As the core of adsorption, various functional adsorbents have been designed to meet the demands of gold recovery, such as metal organic frameworks (MOFs), organic polymers, and biomass materials.[3d,4] However, a majority of these adsorbents suffer from terrible kinetics with several hours or even days to reach equilibrium.[4b-4d] Additionally, the poor selectivity, low loading capacity and lacking stability also go against the efficient recovery of gold. Consequently, it is essential to design novel stable adsorbents with large capacity and rapid kinetics for selective gold recovery.

Typical covalent organic frameworks (COFs) are known as a kind of crystalline porous materials linked with reversible covalent bonds such as boronate ester, boroxine, azine, hydrazone and imine, showing wide potential in gas storage, catalysis, sensing and separation.[5] The relatively stable imine-linked COFs reveal greater promise in diverse fields than the easily hydrolyzed boronate esters or boroxines-linked COFs, indicating the stability plays a pushing role in the application of COFs.[6] However, typical COFs are formed on the basis of dynamic covalent chemistry.[5b,7] The reversible covalent linkage is the nub of the formation of crystallinity as well as the inherent limitation for the stability of COFs.

Construction of COFs with irreversible bonds is crucial in developing stable COFs, but remains challenging. Few efforts have been devoted to explore this likelihood. Polyarylether-based COFs (also called dioxin-linked COFs) have been synthesized with irreversible nucleophilic aromatic substitution reaction.[6a,8] The irreversible benzoxazole- and amide-linked COFs have been prepared via chemical conversion[9] or under high-temperature and high-pressure.[10] However, the available synthetic strategies and the number of irreversible COFs are nowhere near enough for the wide applications.

Herein, we report the design and synthesis of a highly stable and irreversible amide-linked COF JNU-1 for selective gold recovery via building block exchange (BBE). A BBE strategy is developed for the synthesis of JNU-1 owing to its great potential in preparing *de novo* unreachable COFs.[11] Amide linkage is designed as both inherent linkage and functional groups since it is irreversible and selective for gold.[3b,12] The proposed amide-linked JNU-1 is prepared from terephthaloyl chloride (TaCl) and the mother COF TzBA consisting of 4,4',4''-(1,3,5-Triazine-2,4,6-triyl)trianiline (Tz) and 4,4'-biphenyldicarboxaldehyde (BA) via the BBE strategy. The design of such a BBE strategy for the preparation of JNU-1 and its application for gold recovery are studied via detail experimental characterization in combination with quantum mechanics calculations. The prepared JNU-1 gives unprecedented fast kinetics, high selectivity as well as large capacity for gold recovery. This work shows the high potential of introducing irreversible bonds as both inherent linkage and functional groups in preparation of stable COFs for wide significant applications.

[a] Dr. H.-L. Qian, Prof. Dr. X.-P. Yan
State Key Laboratory of Food Science and Technology
Jiangnan University
Wuxi 214122, China
E-mail: xpyan@jiangnan.edu.cn
hlqian@jiangnan.edu.cn
[b] Prof. Dr. X.-P. Yan
International Joint Laboratory on Food Safety
Jiangnan University
Wuxi 214122, China
[c] Dr. H.-L. Qian, F.-L. Meng, Prof. Dr. X.-P. Yan
Institute of Analytical Food Safety, School of Food Science and Technology
Jiangnan University
Wuxi 214122, China
[d] Prof. Dr. X.-P. Yan
Key Laboratory of Synthetic and Biological Colloids, Ministry of Education
Jiangnan University
Wuxi 214122, China
[e] Dr. C.-X. Yang
Research Center for Analytical Sciences, College of Chemistry
Nankai University
Tianjin 300071, China

Supporting information for this article is given via a link at the end of the document.

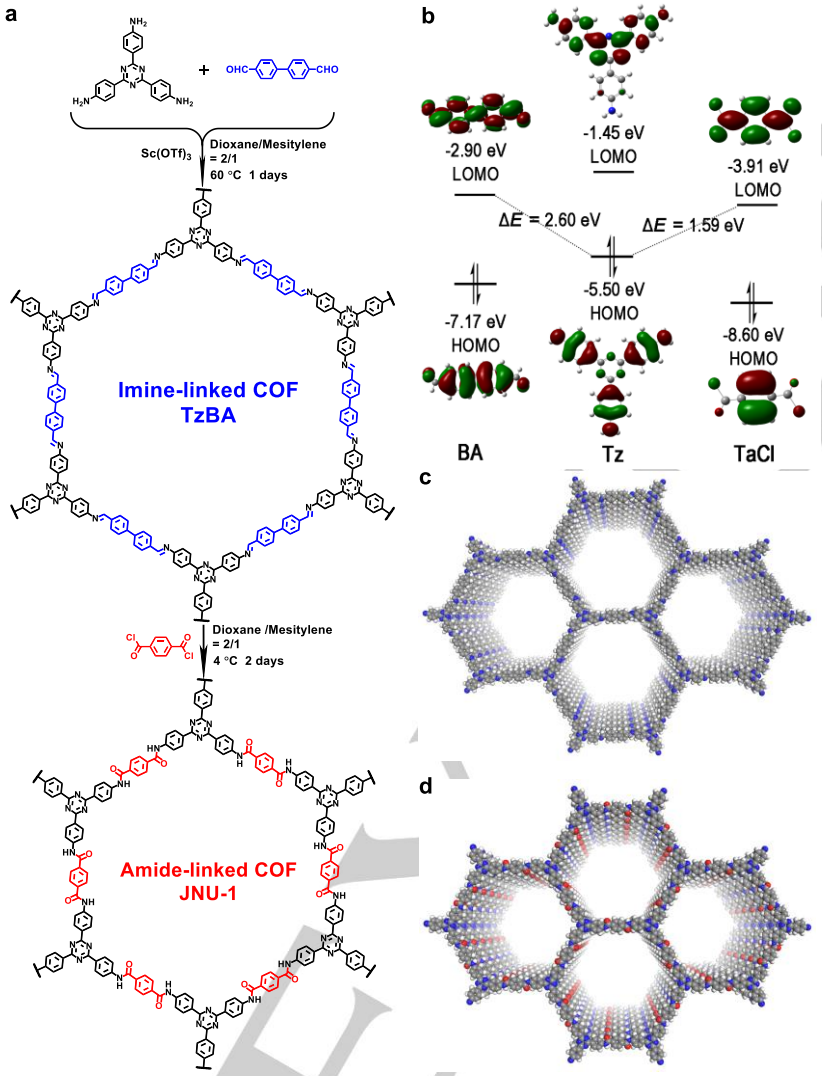

Figure 1. (a) Design of a BBE strategy for the synthesis of JNU-1. (b) Diagram for computed HOMO–LUMO interactions of Tz with BA and TaCl. (c) Space-filling model of TzBA. (d) Space-filling model of JNU-1 (gray, C; blue, N; red, O; white, H).

Results and Discussion

Design and preparation of amide-linked COFs via BBE. Dynamic covalent chemistry is thought to be the fundamental of forming typical crystalline COFs, where the reversible reaction is the key of the process.[5b,7] However, the formed reversible linkage inherently limits the stability of COFs. Fabrication of COFs based on irreversible bonds is an effective way to obtain stable COFs, but hard to access via conventional *de novo* approach. BBE strategy is a promise way to synthesize *de novo* inaccessible COFs,[11] but has never been designed for the preparation of irreversible COFs. Here we show the design and synthesis of highly stable COF based on irreversible linkage via BBE. We took amide-linked COF JNU-1 as a proof-of-concept (Figure 1a). The irreversible amide with high selectivity for gold[3b,12] was selected as the linkage, which is a prerequisite to form stable COFs. However, it is impossible to prepare amide-linked COF JNU-1 via direct condensation of acyl chloride and amine monomer, as confirmed by the powder X-ray diffraction (PXRD) (Figure S1a, c and d). So, in the present designed BBE strategy (Figure 1a), Tz was firstly condensed with BA to prepare the crystalline mother COF TzBA. Note that scandium(III) trifluoromethanesulfonate ($Sc(OTf)_3$) was used to replace typical aqueous acetic acid as the catalyst due to the negative influence of H_2O in aqueous acetic acid on the chloride monomer in next BBE step. Terephthaloyl chloride (TaCl) with higher nucleophilicity was chosen to exchange the BA block of TzBA to produce the daughter JNU-1 as the easiness of a chemical reaction is mainly determined by the electron delocalization between the HOMO and LUMO based on the frontier orbit theory.[13] As shown in Figure 1b, the energy gap between the HOMO of Tz and the LUMO of TaCl ($\Delta E_{HOMO(Tz)-LOMO(TaCl)}$) is lower than $\Delta E_{HOMO(Tz)-LOMO(BA)}$, so the electron is easier to flow from the HOMO of Tz to the LUMO of TaCl than to the LUMO of BA

Control of reaction rate is essential for BBE. Rapid reaction is unfavorable for the formation of high crystallinity,[14] so we

investigated the effect of the amount of TaCl, reaction temperature and time on the crystallinity of the prepared JNU-1. The results show that 87.1% of TzBA was converted into high-crystalline JNU-1 with 1 equiv TaCl for BBE in the absence of triethylamine (TEA) at low temperature (0 and 4 °C) for 2 days (Figures S2-S6).

Characterization of amide-linked COF. The simultaneous disappearance of amino and aldehyde stretching bands for the starting monomers as well as the appearance of imine stretching band for TzBA in Fourier transform infrared (FTIR) spectra indicate the successful condensation of Tz and BA (Figure S7). The prepared mother COF TzBA gave the XRD pattern with several main diffraction peaks at 2.41°, 4.11° and 6.09°, in good agreement with the corresponding simulated one (Figures S8 and S9, Table S1). These results show the designable crystallinity and structure of TzBA. Compared to its mother COF TzBA, the BBE product JNU-1 exhibited an extraordinary improvement in crystallinity as the intensity of main peak at 2.40° increased about 10 times (Figure 2a). The as-prepared JNU-1 also gave several diffraction peaks at 4.10°, 4.69°, 6.14° and 26.07° (Figure S1b). The PXRD pattern of the as-prepared JNU-1 coincided well with that of simulated AA stacking unite cell of JNU-1 (a = b = 43.0452 Å, c = 3.3639 Å, α = β =90° and γ = 120°) with Rwp of 6.79% and Rp of 5.35% after Pawley refinement, rather than that of simulated AB stacking model (Figure 2b-2d and Figure S10). The unit cell parameters of JNU-1 show little change after the BBE of TaCl, revealing the overall structure retained (Tables S1-S2). In addition, the PXRD pattern of control COF exhibited no improvement without addition of TaCl (Figure. S11). The above PXRD data confirm the transformation of TzBA to JNU-1 after BBE with TaCl.

The transformation of TzBA to designable JNU-1 in the presence of TaCl was further verified by FTIR and ^{13}C solid-state nuclear magnetic resonance (SNMR) spectroscopy. The appearance of a distinct stretching band at 1656 cm^{-1} (corresponding to the C=O of amide) in accompany with the absence of the C=N stretching band at 1621 cm^{-1} in the FTIR spectra of the as-prepared JNU-1 indicate the conversion of imine into amide after BBE (Figure 3a, Figure S12). The mother COF TzBA gave a wide peak at 156 ppm for imine carbon in the ^{13}C SNMR spectra (Figure S13). In contrast, the BBE product JNU-1 gave a new peak for amide carbon at 168 ppm instead of imine carbon, which was verified by the amide carbon peak at 166 ppm in ^{13}C SNMR spectra of model compound (Figure 3b, Figures S14-S17). All the above evidences further confirm the formation of amide-linkage.

Scanning electron microscopy (SEM) images demonstrate no clear change in morphology during the transformation of TzBA to JNU-1. Both TzBA and JNU-1 exhibited the aggregation of spheres (Figure S18). Transmission electron microscopy (TEM) images show typical layer-like structure of the two COFs, coinciding with the simulated stacking layer structure (Figure S19). TzBA and JNU-1 gave Brunauer–Emmett–Teller (BET) surface area of 156 and 261 $m^2\ g^{-1}$ with the pore size of *ca.* 40 and 39 Å, and the pore volume of 0.36 and 0.70 $cm^3\ g^{-1}$, respectively (Figure S20). The increase of the BET surface area may come from the improvement of the crystallinity, the decrease of the pore size and the increased pore volume due to the reduction in the building unit size after BBE. On the contrary, the TzTaCl prepared from the direct condensation of TaCl and Tz gave the BET surface area of only 33 $m^2\ g^{-1}$ with no obvious pores (Figure S20).

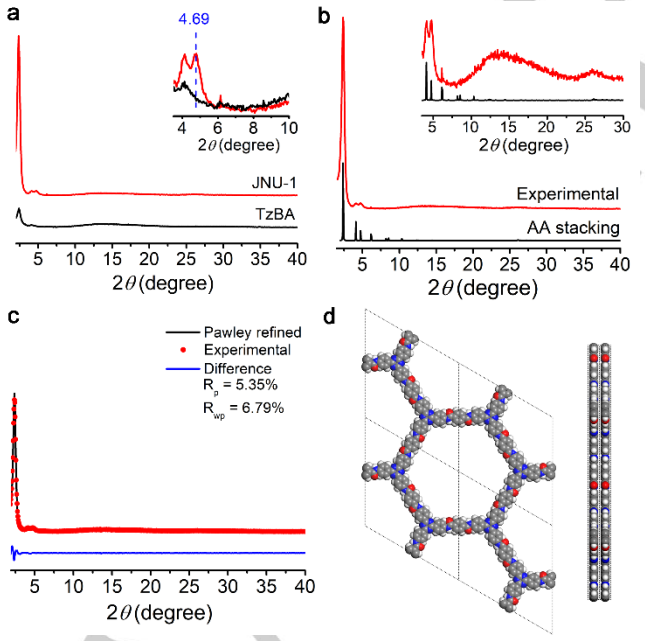

Figure 2. (a) PXRD patterns of the mother COF TzBA and its BBE product JNU-1. (b) Experimental and simulated PXRD patterns (AA stacking) of JNU-1. (c) Pawley refinement of JNU-1. (d) Eclipsed AA unit cell of JNU-1.

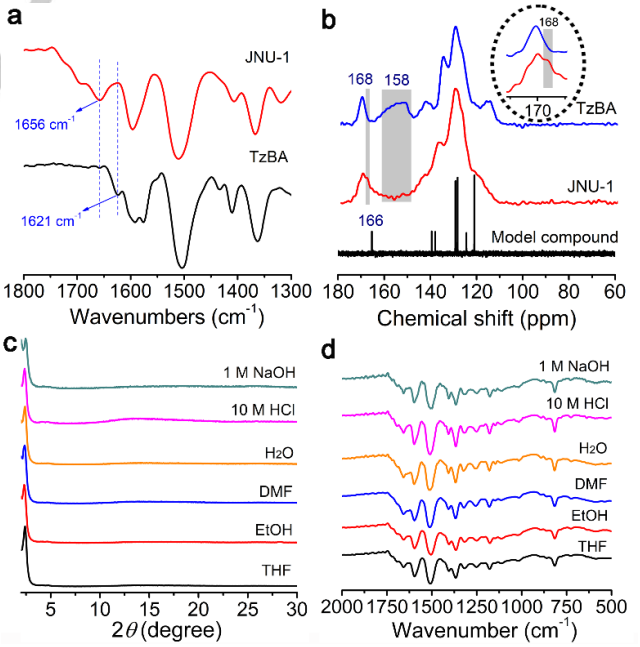

Figure 3. (a) FTIR spectra of TzBA and its BBE product JNU-1. (b) Liquid 13C NMR spectra of model compound and the 13C SNMR spectrum of TzBA and its BBE product JNU-1. (c) PXRD patterns and (d) FTIR spectra of JNU-1 after treatment with various solvents.

Stability of the amide-linked COF JNU-1. Conversion of reversible imine linkage in TzBA to irreversible amide linkage in JNU-1 greatly enhanced the stability of COFs. The chemical stability was investigated by exposing the COFs to various media including tetrahydrofuran (THF), ethanol (EtOH), dimethylformamide (DMF), water, HCl and NaOH for 1 day, and monitoring the change of the PXRD patterns and FTIR spectra. The crystallinity and skeleton of the amide-linked COF JNU-1 still remained in various organic solvents, 10 M HCl and 1 M NaOH due to no obvious change in the PXRD pattern and FTIR spectra for JNU-1 (Figure 3c and 3d), revealing the high chemical stability (especially acid stability) of JNU-1 compared to many reported COFs (Table S3). In contrast, the loss of the main diffraction peaks in the PXRD pattern in conjunction with the appearance of aldehyde peak at 1698 cm^{-1} in the FTIR spectra for TzBA after the treatment of 2 M HCl and 1 M NaOH indicate the hydrolysis of the imine and the framework destruction in TzBA (Figures S21 and S22). However, both TzBA and JNU-1 own excellent thermal stability up to 400 °C (Figure S23). The excellent stability in combination of the amide linkage makes JNU-1 great potential for gold recovery from harsh solutions.

JNU-1 for gold adsorption and recovery. The irreversible amide not only serves as the linkage, but also as the functional groups to bring the JNU-1 with the ability for effective gold recovery. So, we studied the adsorption performance of JNU-1 for the recovery of Au(III). The optimal acidity for the absorption of Au(III) was 2 mol L^{-1} HCl (Figure S24), which gave no effect on the structure of JNU-1 due to its high stability under strong acidity (Figure 3c and 3d). In contrast, the imine-linked TzBA was incompetent under such strong acidity (Figures S21 and S22). The adsorption of Au(III) followed the pseudo-second-order kinetic model (Supporting methods, Figure S25 and Table S4) and reached equilibrium in only 10 sec (Figure 4a and Figure S26). To the best of our knowledge, JNU-1 offers the fastest kinetics for the adsorption of Au(III), in contrast to previous adsorbents on which several hours or even days were needed for the adsorption of Au(III) to reach equilibrium (Table S5). Such ultrafast adsorption is mainly attributed to the inherent amide linkage of the ordered COF structure as the functional group rather than the modification in the channel or pore.

The adsorption isotherms were well fitted with the Langmuir model (R^2 > 0.997), revealing the dominant monolayer adsorption of Au(III) on JNU-1 (Figure 4b, Supporting methods and Table S6).[15] The Langmuir constant K_L decreased as temperature increased, indicating the affinity of protonated amides to Au(III) was refrained by thermal energy. The calculated maximum adsorption capacity (q_m) was 1124 ± 10 mg g^{-1}, larger than most of previous absorbents for Au(III) including MOFs, organic polymers, nanoparticles and TzTaCl (Table S5). Although biomaterials such as cross-linked orange juice residue and thiosemicarbazide functionalized corn bract gave larger capacity, their adsorption kinetics was extremely slower than JNU-1 (Table S5). In addition, TzTaCl gave poor performance for gold recovery with slow kinetics and low adsorption capacity,

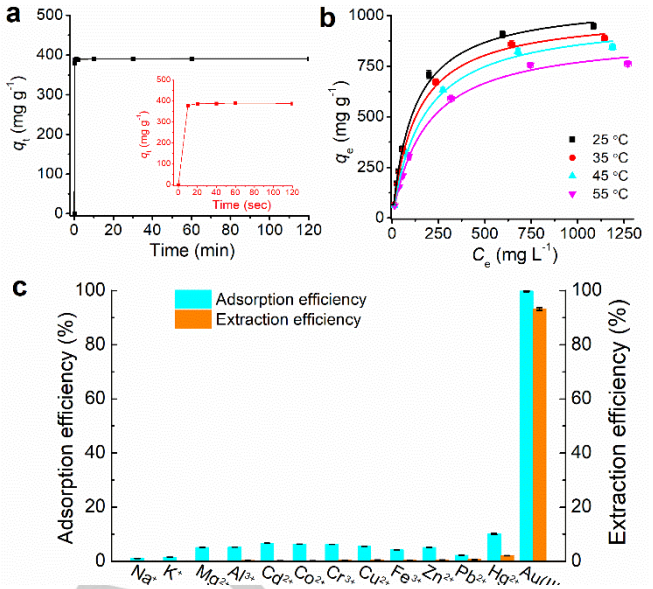

Figure 4. (a) Time-dependent adsorption of gold at initial concentration of 396 mg L^{-1}. (b) Adsorption isotherms of gold in the initial concentration range of 72-2030 mg L^{-1} at a predetermined temperature (35-55 °C). (c) Adsorption (cyan) and extraction (orange) efficiency of metals on the JNU-1. Initial concentration (mg L^{-1}): Na^+, 502.5; K^+, 501.8; Mg^{2+}, 509.5; Al^{3+}, 499.2; Cd^{2+}, 519.3; Co^{2+}, 481.0; Cr^{3+}, 503.6; Cu^{2+}, 504.8; Fe^{3+}, 499.4; Zn^{2+}, 479.1; Pb^{2+}, 510.6; Hg^{2+}, 504.5; Au(III), 4.68. q_t is the adsorption capacity at a predetermined time, q_e is the equilibrium adsorption capacity and C_e is the equilibrium concentration.

further proving the necessity of the preparation of JNU-1 via BBE for high superiority gold recovery (Figure S27; Table S5).

It is crucial for the designed adsorbent to selectively adsorb the specific target in the presence of potential competing species. JNU-1 adsorbed 99.8% of Au(III) in 10 sec even in the presence of 100 times higher concentration of potential competing metal ions (Na^+, K^+, Mg^{2+}, Al^{3+}, Cd^{2+}, Co^{2+}, Cr^{3+}, Cu^{2+}, Fe^{3+}, Zn^{2+}, Pb^{2+} and Hg^{2+}), but only 1.0%-10.1% of the competing metal ions (Figure 4c, Table S7). Rinsing the metal-adsorbed JNU-1 with water before desorption removed 79.5-98.8% of the competing ions from JNU-1, but led to very little loss of Au(III) (6.6%) due to the high affinity of JNU-1 to Au(III). Further desorption with thiourea solution gave the extraction efficiency of 93.2% for Au(III), but only 0.03%-2.1% for the competing metal ions. Two adsorption-rinsing-desorption cycles gave high purity of gold (96.3%) (Figure S28). The high selectivity of JNU-1 for Au(III) resulted from the strong affinity of amides in JNU-1 to Au(III). The amide group of JNU-1 was protonated to form $H[JNU-1]^+$. $[AuCl_4]^-$ was dynamically assembled with the protonated amide $H[JNU-1]^+$ via the dominant hydrogen interaction (for more details, please see the following section), leading to strong adsorption of Au(III) on JNU-1. In contrast, the potential coexisting metals mainly appeared as cations rather than chloride anions in 2 mol L^{-1} HCl, giving low interference with the adsorption of $[AuCl_4]^-$. Considering the obvious merits of ultrafast kinetics, large capacity and high selectivity, JNU-1 should be an outstanding candidate for gold recovery.

Efficient desorption of Au(III) from JNU-1 is essential to the reusability of the prepared COF. Thiourea was employed to desorb Au(III) for its great affinity to gold. About 97% of Au(III) was desorbed from JNU-1 with a mixture solution of 1 mol L^{-1} thiourea and 1 mol L^{-1} HCl solution in 5 min (Figure S29) due to the liable formation of strong cation complex from Au and thiourea in acid solution.[16] Neutral (H_2O), and basic condition (1 mol L^{-1} NaOH) were unfavorable for the desorption (Figure S30). The crystalline structure of JNU-1 remained after the adsorption and desorption process (Figure S31). The regenerated COF still gave more than 85% adsorption efficiency for Au(III) after three adsorption-desorption cycles (Figure S32), suggesting the good reusability of JNU-1.

Adsorption Mechanism. Thermodynamic study and quantum mechanics calculation in conjunction with experimental characterization were performed to further understand the adsorption mechanism. The thermodynamic parameters were first determined for the adsorption of Au(III) on JNU-1 (Supporting methods). The adsorption of Au(III) was proceeded spontaneously ($\Delta G < 0$) and enthalpy-driven ($\Delta H < 0$, $\Delta S < 0$) (Table S8). The negative ΔH and ΔS indicate the adsorption of Au(III) on JNU-1 was an exothermic process with increased order owing to the adsorption of $[AuCl_4]^-$ onto the JNU-1 in the solution.

XPS spectra of N, O, Au and Cl, before and after the adsorption of Au(III) on JNU-1 were compared to reveal the active adsorption sites of JNU-1 for Au(III). Au 4f peaks evidently appeared in the wide XPS scanning spectra for Au(III) adsorbed JNU-1 after (JNU-1-Au(III)) (Figure S33). The characteristic peaks of N 1s for NH (398.3 eV), C=N (399.6 eV) and $C=N^+$ (402.5 eV) of JNU-1[17] did not change after the absorption of Au(III), indicating the absence of N in the adsorption (Figure. 5a). The binding energy of O 1s for C=O and protonated $C=OH^+$ slightly shifted from 530.8 and 531.5 eV to 531.1 and 531.8 eV, respectively. The protonation of amide in JNU-1 was in equilibrium. The interaction of $[AuCl_4]^-$ with the $C=OH^+$ in the protonated amide made the original equilibrium shift from C=O to $C=OH^+$, leading to the increased peak area of $C=OH^+$ in company with the decreased peak area of C=O in XPS spectra (Figure. 5b). Meanwhile, the binding energy of Au(III) 4f shifted to lower position compared with that of Au(III) before adsorption (Figure. 5c). Furthermore, the electron paramagnetic resonance (EPR) peak area for JNU-1 evidently decreased after the adsorption of Au(III) (Figure S34). The above results imply the interaction between the Au and O.[18] The line shape of the Cl 2p spectrum for Au(III) appeared difference after it was absorbed on the JNU-1 (Figure 5d). The Cl 2p signals at 196.5 eV, 197. eV and 199.3 eV were assigned to chloride anion (Cl^-), chlorine anion under more positive condition (Cl*), and Au-Cl, respectively.[17,19] After the loading of Au(III) on the JNU-1, the binding energy of Cl 2p for Au-Cl (199.3 eV) significantly shifted to 201.2 eV, showing the main attribution of Au-Cl···H to the adsorption. Element mapping shows the uniform distribution of evident amounts of Au(III) in JNU-1, owing to the inherent linkage of amide for the ordered COF structure (Figure S35). All the above results verified the main attendance of amide in the adsorption of Au(III).

Quantum mechanics calculation with density functional theory (DFT) method was performed to get further insight into the active binding sites and the interactions between JNU-1 and Au(III) (as $[AuCl_4]^-$).[20] Considering the structure of JNU-1, three possible active sites including $C=NH^+$, $C=OH^+$ and N-H likely

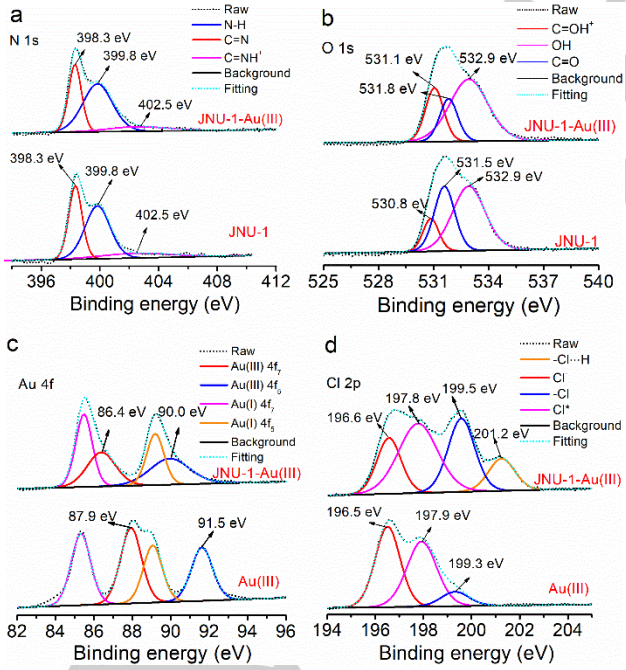

Figure 5. (a), (b) XPS spectra of N 1s and O 1s for JNU-1 before and after the adsorption of Au(III). (c), (d) XPS spectra of Au 4f and Cl 2p for Au(III) before and after the adsorption on JNU-1.

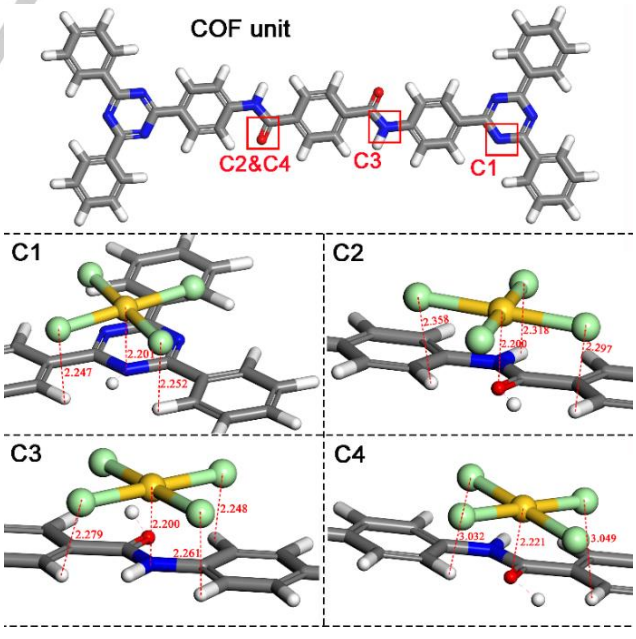

Figure 6. Optimized geometries of the C1-C4 configurations corresponding to the interaction of different binding sites with Au(III) as $[AuCl_4]^-$ (Gray, C; blue, N; red, O; white, H; yellow, Au; green Cl, distance unit, Å).

interact with $[AuCl_4]^-$ in acid condition. Hence, four configurations (C1-C4) were constructed for the interactions between these three active sites and $[AuCl_4]^-$ to optimize their geometry based on DFT (Figure 6). The corresponding adsorption energies (E_{ad}) of C1-C4 were calculated with equation 1 (Supporting methods, Table 1). The C1-C3 configurations were considered for potential hydrogen bonding and coordinate interaction of the active site $C=NH^+$, $C=OH^+$ and N-H with $[AuCl_4]^-$, respectively. The average distances of C(N)-H···Cl (2.25-2.32 Å) in C1-C3 after optimization confirmed the hydrogen bonding, while that of N(O)···Au (2.20 Å) proved the coordinate interaction. Moreover, the C2 configuration with two C-H···Cl, one N-H···Cl and one C=O→Au gave more negative adsorption energy ($E_{ad,}$ −164.5 kcal mol^{-1}) than the configurations of C1 (−151.3 kcal mol^{-1}) with two C-H···Cl and one C=N→Au, and C3 with three C-H···Cl and one C-N→Au (−141.8 kcal mol^{-1}), indicating that $[AuCl_4]^-$ tends to bind with the $C=OH^+$ through hydrogen bonding and coordinate interaction. In order to investigate the dominant interaction between $C=OH^+$ and $[AuCl_4]^-$, we adjusted the position of $[AuCl_4]^-$ in C2 to form a new configuration (C4). The similar average length of Au-O in C2 and C4 means the coordinate interaction is unchanged, while the average length of the hydrogen bond in C4 (3.04 Å) was much longer than C2 (2.32 Å), indicating the weaker hydrogen interaction in C4.[21] Correspondingly, the E_{ad} of C4 configuration gave a significant decrease to -73.2 kcal mol^{-1} in comparison with the C2 configuration (E_{ad}, -164.5 kcal mol^{-1}), revealing that the dominant hydrogen bonds C-H···Cl and N-H···Cl in conjunction with coordinate interaction between Au-O are responsible for the adsorption of Au(III) on JNU-1, which is in agreement with XPS result. Moreover, the low capacity and selectivity of the imine linked TzBA for Au(III) also conveyed the vital significance of the amide in JNU-1 for the recovery of gold (Figure S36).

Table 1. Calculated results for the C1-C4 configurations for possible interactions between three active sites and $[AuCl_4]^-$ by DFT

Configuration	Active site	Average distance (Å)		Indicative interaction	E_{ad} (kcal mol^{-1})
		C(N)-H···Cl	N(O)→Au		
C1	$C=NH^+$	2.25	2.20	hydrogen and coordinate interaction	-151.3
C2	$C=OH^+$	2.32	2.20	hydrogen and coordinate interaction	-164.5
C3	N-H	2.26	2.20	hydrogen and coordinate interaction	-141.8
C4	$C=OH^+$	3.04	2.22	hydrogen and coordinate interaction	-73.2

Conclusion

In conclusion, we have shown the design and preparation of a highly stable COF JNU-1 based on irreversible amide linkage for ultrafast and selective recovery of gold. Introducing irreversible linkage to COF structure is a promising way to the preparation of stable COFs, but it is difficult to access stable COFs based on irreversible linkage via conventional *de novo* approach. We have displayed the great potential of BBE in the preparation of highly stable irreversible COFs using amide-linked JNU-1 as an example. The irreversibility and selectivity of amide linkage to gold is the prerequisite for the design of highly stable JNU-1 for effective gold recovery. The protonated amide linkage in the well-ordered COF networks strongly assembles with $[AuCl_4]^-$ via the dominant hydrogen interaction of C-H···Cl and N-H···Cl in conjunction with coordinate interaction of Au and O, rendering JNU-1 ultrafast kinetics, excellent selectivity and large adsorption capacity for gold recovery. We believe this study will largely promote the preparation and exploration of the potential of functional irreversible COFs in diverse applications.

Acknowledgements

This work was supported by the National Natural Science Foundation of China (No. 21804055 and 21775056), the Natural Science Foundation of Jiangsu Province (No. BK20180585), the China Post-doctoral Science Foundation (No. 2018M630510), the National First-class Discipline Program of Food Science and Technology (No. JUFSTR20180301), the Fundamental Research Funds for Central Universities (Grant JUSRP51714B), the Program of "Collaborative Innovation Center of Food Safety and Quality Control in Jiangsu Province".

Keywords: Building block exchange • irreversible linkage• covalent organic frameworks • gold recovery

[1] S. J. H. Syed, *Hydrometallurgy* **2012**, *115*, 30-51.

[2] a) Y. Ding, S. Zhang, B. Liu, H. Zheng, C.-c. Chang, C. Ekberg, *Resour. Conserv. Recy.* **2019**, *141*, 284-298; b) J. Cui, L. Zhang, *J. Hazard. Mater.* **2008**, *158*, 228-256.

[3] a) W. A Matthew, P. J. Bailey, P. A. Tasker, J. R. Turkington, R. A. Grant, J. B. Love, *Chem. Soc. Rev.* **2014**, *45*, 123-134; b) E. D. Doidge, I. Carson, P. A. Tasker, R. J. Ellis, C. A. Morrison, J. B. Love, *Angew. Chem. Int. Ed.* **2016**, *55*, 12436-12439; c) A. Yoshimura, M. Takai, Y. J. H. Matsuno, *Hydrometallurgy* **2014**, *149*, 177-182; d) M. Mon, J. Ferrando-Soria, T. Grancha, F. R. Fortea-Perez, J. Gascon, A. Leyva-Perez, D. Armentano, E. Pardo, *J. Am. Chem. Soc.* **2016**, *138*, 7864-7867; e) H. Murakami, S. Nishihama, K. J. H. Yoshizuka, *Hydrometallurgy* **2015**, *157*, 194-198.

[4] a) C. Wang, G. Lin, J. Zhao, S. Wang, L. Zhang, Y. Xi, X. Li, Y. Ying, *Chem. Eng. J.* **2020**, *380*, 120674; b) Y. Ganchimeg, G. Burmaa, K. Naoki, K. Hee Joon, *J. Chem. Chem. Eng.* **2017**, *11*, 15-21; c) J. R. Dodson, H. L. Parker, A. M. García, A. Hicken, K. Asemave, T. J. Farmer, H. He, J. H. Clark, A. J. Hunt, *Green Chem.* **2015**, *17*, 1951-1965; d) K. Inoue, D. Parajuli, M. Gurung, B. Pangeni, K. Khunathai, K. Ohto, H. Kawakita, IntechOpen, **2019**.

[5] a) A. P. Côté, A. I. Benin, N. W. Ockwig, M. O'Keeffe, A. J. Matzger, O. M. Yaghi, *Science* **2005**, *310*, 1166-1170; b) X. Feng, X. Ding, D. Jiang, *Chem. Soc. Rev.* **2012**, *41*, 6010-6022; c) S. Y. Ding, W. Wang, *Chem. Soc. Rev.* **2013**, *42*, 548-568; d) P. J. Waller, F. Gandara, O. M. Yaghi, *Acc. Chem. Res.* **2015**, *48*, 3053-3063; e) C. S. Diercks, O. M. J. S. Yaghi, *Science* **2017**, *355*, eaal1585; f) N. Huang, P. Wang, D. Jiang,

Nat. Rev. Mater. **2016**, *1*, 16068; g) H. L. Qian, C. X. Yang, W. L. Wang, C. Yang, X. P. Yan, *J. Chromatogr. A* **2018**, *1542*, 1-18; h) L. He, S. Liu, L. Chen, X. Dai, J. Li, M. Zhang, F. Ma, C. Zhang, Z. Yang, R. Zhou, Z. Chai, S. Wang, *Chem. Sci.* **2019**, *10*, 4293-4305.

[6] a) X. Guan, H. Li, Y. Ma, M. Xue, Q. Fang, Y. Yan, V. Valtchev, S. Qiu, *Nat. Chem.* **2019**, *11*, 587-594; b) Q. Lu, Y. Ma, H. Li, X. Guan, Y. Yusran, M. Xue, Q. Fang, Y. Yan, S. Qiu, V. Valtchev, *Angew. Chem. Int. Ed.* **2018**, *57*, 6042-6048; c) P. F. Wei, M. Z. Qi, Z. P. Wang, S. Y. Ding, W. Yu, Q. Liu, L. K. Wang, H. Z. Wang, W. K. An, W. Wang, *J. Am. Chem. Soc.* **2018**, *140*, 4623-4631; d) A. Halder, S. Karak, M. Addicoat, S. Bera, A. Chakraborty, S. H. Kunjattu, P. Pachfule, T. Heine, R. Banerjee, *Angew. Chem. Int. Ed.* **2018**, *57*, 5797-5802; e) P.-L. Wang, S.-Y. Ding, Z.-C. Zhang, Z.-P. Wang, W. Wang, *J. Am. Chem. Soc.* **2019**, *141*, 18004-18008; f) S. Chandra, S. Kandambeth, B. P. Biswal, B. Lukose, S. M. Kunjir, M. Chaudhary, R. Babarao, T. Heine, R. Banerjee, *J. Am. Chem. Soc.* **2013**, *135*, 17853-17861.

[7] S. J. Rowan, S. J. Cantrill, G. R. Cousins, J. K. Sanders, J. F. Stoddart, *Angew. Chem. Int. Ed.* **2002**, *41*, 898.

[8] B. Zhang, M. Wei, H. Mao, X. Pei, S. A. Alshmimri, J. A. Reimer, O. M. Yaghi, *J. Am. Chem. Soc.* **2018**, *140*, 12715-12719.

[9] a) P. J. Waller, S. J. Lyle, T. M. Osborn Popp, C. S. Diercks, J. A. Reimer, O. M. Yaghi, *J. Am. Chem. Soc.* **2016**, *138*, 15519-15522; b) P. J. Waller, Y. S. AlFaraj, C. S. Diercks, N. N. Jarenwattananon, O. M. Yaghi, *J. Am. Chem. Soc.* **2018**, *140*, 9099-9103.

[10] D. Stewart, D. Antypov, M. S. Dyer, M. J. Pitcher, A. P. Katsoulidis, P. A. Chater, F. Blanc, M. J. Rosseinsky, *Nat. Commun.* **2017**, *8*, 1102.

[11] H.-L. Qian, Y. Li, X.-P. Yan, *J. Mater. Chem. A* **2018**, *6*, 17307-17311.

[12] a) E. A. Mowafy, D. Mohamed, *Sep. Purif. Technol.* **2016**, *167*, 146-153; b) J. S. Preston, A. C. du Preez, *Solvent Extr. Ion Exch.* **1995**, *13*, 391-413.

[13] a) K. J. s. Fukui, *Science* **1982**, *218*, 747-754; b) J. Zhou, L. L. Liu, L. L. Cao, D. W. Stephan, *Angew. Chem. Int. Ed.* **2018**, *57*, 3322-3326.

[14] X. Feng, L. Chen, Y. Dong, D. Jiang, *Chem. Commun.* **2011**, *47*, 1979-1981.

[15] J. Q. Jiang, C. X. Yang, X. P. Yan, *ACS Appl. Mater. Interfaces* **2013**, *5*, 9837-9842.

[16] M. Gurung, B. B. Adhikari, H. Kawakita, K. Ohto, K. Inoue, S. Alam, *Hydrometallurgy* **2013**, *133*, 84-93.

[17] K. G. Neoh, T. T. Young, N. T. Looi, E. T. Kang, K. L. Tan, *Chem. Mater.* **1997**, *9*, 2906-2912.

[18] J. Li, C.-y. Liu, Y. Liu, *J. Mater. Chem.* **2012**, *22*, 8426-8430.

[19] E. T. Kang, Y. P. Ting, K. L. Tan, *J. Appl. Polym. Sci.* **1994**, *53*, 1539-1545.

[20] a) H. Hassan, R. Heidar, *J. Phys. D: Appl. Phys.* **2018**, *51***,** 34540; b) J. Yoo, S.-J. Cho, G. Y. Jung, S. H. Kim, K.-H. Choi, J.-H. Kim, C. K. Lee, S. K. Kwak, S.-Y. J. N. l. Lee, *Nano Lett.* **2016**, *16*, 3292-3300.

[21] Y. Li, J. Wu, D. Cao, J. Wang, *J. Phys. Chem. A* **2016**, *120*, 8444-8449.

Entry for the Table of Contents

Layout 1:

RESEARCH ARTICLE

An irreversible amide-linked COF was designed and synthesized via a building block exchange strategy for efficient recovery of gold. The irreversible amide linked COF gave good stability, unprecedented fast kinetics, excellent selectivity and outstanding adsorption capacity for gold recovery.

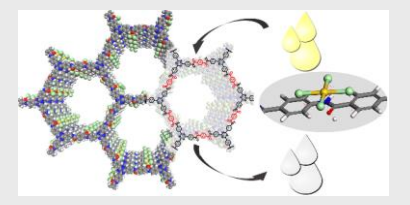

H.-L. Qian, F.-L. Meng, C.-X. Yang, and X-P Yan**

Page No. – Page No.

Irreversible amide-linked covalent organic framework for selective and ultrafast gold recovery